Two Groups Control Light-Induced Schiff Base Deprotonation and the Proton Affinity of Asp^{85} in the Arg^{82}His Mutant of Bacteriorhodopsin

Eleonora S. Imasheva,* Sergei P. Balashov,* Thomas G. Ebrey,* Ning Chen,# Rosalie K. Crouch,# and Donald R. Menick#

*Center for Biophysics and Computational Biology and Departments of Cell and Structural Biology and Biochemistry, University of Illinois at Urbana-Champaign, Urbana, Illinois 61801, and #Medical University of South Carolina, Charleston, South Carolina 29425 USA

ABSTRACT Arg^{82} is one of the four buried charged residues in the retinal binding pocket of bacteriorhodopsin (bR). Previous studies show that Arg^{82} controls the pK_as of Asp^{85} and the proton release group and is essential for fast light-induced proton release. To further investigate the role of Arg^{82} in light-induced proton pumping, we replaced Arg^{82} with histidine and studied the resulting pigment and its photochemical properties. The main pK_a of the purple-to-blue transition (pK_a of Asp^{85}) is unusually low in R82H: 1.0 versus 2.6 in wild type (WT). At pH 3, the pigment is purple and shows light and dark adaptation, but almost no light-induced Schiff base deprotonation (formation of the M intermediate) is observed. As the pH is increased from 3 to 7 the M yield increases with pK_a 4.5 to a value ~40% of that in the WT. A transition with a similar pK_a is observed in the pH dependence of the rate constant of dark adaptation, k_{da}. These data can be explained, assuming that some group deprotonates with pK_a 4.5, causing an increase in the pK_a of Asp^{85} and thus affecting k_{da} and the yield of M. As the pH is increased from 7 to 10.5 there is a further 2.5-fold increase in the yield of M and a decrease in its rise time from 200 μs to 75 μs with pK_a 9.4. The chromophore absorption band undergoes a 4-nm red shift with a similar pK_a. We assume that at high pH, the proton release group deprotonates in the unphotolyzed pigment, causing a transformation of the pigment into a red-shifted "alkaline" form which has a faster rate of light-induced Schiff base deprotonation. The pH dependence of proton release shows that coupling between Asp^{85} and the proton release group is weakened in R82H. The pK_a of the proton release group in M is 7.2 (versus 5.8 in the WT). At pH < 7, most of the proton release occurs during O $\rightarrow$ bR transition with $\tau \approx 45$ ms. This transition is slowed in R82H, indicating that Arg^{82} is important for the proton transfer from Asp^{85} to the proton release group. A model describing the interaction of Asp^{85} with two ionizable residues is proposed to describe the pH dependence of light-induced Schiff base deprotonation and proton release.

INTRODUCTION

Light energy transduction in the photochemical cycle of bacteriorhodopsin (Oesterhelt and Stoeckenius, 1971) proceeds through a number of spectroscopically distinct states of the chromoprotein: bR $\rightarrow$ K $\leftrightarrow$ L $\leftrightarrow$ M $\leftrightarrow$ N $\leftrightarrow$ O $\rightarrow$ bR (Lozier et al., 1975; Mathies et al., 1991; Ebrey, 1993; Lanyi, 1993; Lanyi and Váró, 1995). This process is initiated by all-*trans* $\rightarrow$ 13-*cis* photoisomerization of the chromophore in the bR $\rightarrow$ K photoreaction that induces conformational changes in the protein and intramolecular proton transfer from the Schiff base to the internal proton acceptor, Asp^{85}, during the L $\rightarrow$ M conversion and subsequent fast release of a proton to the extracellular surface of the membrane from the proton release group (Siebert et al., 1982; Zimányi et al., 1992; Ebrey, 1993). The second part of the photocycle involves reprotonation of the Schiff base from the internal proton donor Asp^{96} (Rothschild, 1992; Otto et al., 1989; Gerwert et al., 1989) during the M $\rightarrow$ N transition, uptake of a proton at the cytoplasmic surface of the membrane, and reisomerization of the chromophore in the N $\rightarrow$ O transition. In the final step (O $\rightarrow$ bR) of the photocycle, proton transfer from Asp^{85} to the proton release group takes place (Kandori et al., 1997; Balashov et al., 1999).

This basic sequence of events may be altered at high or low pH and by mutation of certain residues. The most sensitive step is the proton release coupled to the proton transfer from the Schiff base to Asp^{85}. In the WT, at neutral pH, light-induced proton transfer from the Schiff base to Asp^{85} during the L-to-M transition results in almost simultaneous proton release to the surface (Liu et al., 1990; Heberle and Dencher, 1992; Cao et al., 1995). The source of the proton is the so-called proton release group, which most likely is not a single residue but rather a complex of residues that includes Glu^{204} (Brown et al., 1995a; Govindjee et al., 1996), Glu^{194} (Balashov et al., 1997; Dioumaev et al., 1998), and water molecules (Luecke et al., 1999). Using two different methods to titrate Asp^{85}, by direct absorption measurements and by the measurements of pH dependence of the thermal isomerization of the chromophore, which is catalyzed by protonation of Asp^{85}, we showed that there is a coupling between the protonation states of Asp^{85} and the proton release group (Balashov et al., 1993, 1995, 1996). Protonation of Asp^{85} lowers the pK_a of the proton release group and, vice versa, deprotonation of the proton release group increases the proton affinity of Asp^{85}. Below pH 5 protonation of Asp^{85} does not lower the pK_a of the proton release group enough to allow it to deprotonate as M is formed (Zimányi et al., 1992); in this case proton release is delayed until the O $\rightarrow$ bR transition (Dencher and Wilms,

Received for publication 19 April 1999 and in final form 1 August 1999.

Address reprint requests to Dr. Thomas G. Ebrey, Departments of Cell and Structural Biology and Biochemistry, University of Illinois at Urbana-Champaign, B107 CLSL, 601 S. Goodwin Ave., Urbana, IL 61801. Tel.: 217-333-2015. Fax: 217-244-6615. E-mail: t-ebrey@uiuc.edu.

0006-3495/99/11/2750/14 $2.00

1975). It occurs from the proton release group (Balashov et al., 1999) and is followed by proton transfer from Asp^{85} to the proton release group (Hessling et al., 1993; Kandori et al., 1997), which resets the protonated state of this group. At pH > 10 the proton release group is already deprotonated in the pigment's initial state ($pK_a \sim 9.5$), so the normal, fast proton release is abolished (Kono et al., 1993); presumably a proton is released from Asp^{85} at the end of the photocycle (Balashov et al., 1996; Dioumaev et al., 1998).

In the initial (unphotolyzed) state, the pK_a of the Schiff base is ~12, whereas the pK_a of Asp^{85} is 2.6. To accomplish proton transfer from the Schiff base to Asp^{85}, the pK_a of the Schiff base should decrease and the pK_a of Asp^{85} should increase during the photocycle. Recent estimates show that indeed the pK_a of Asp^{85} increases up to 10.5 in M (Braiman et al., 1996). The changes in the pK_a of the Schiff base and Asp^{85} after photoisomerization of the chromophore are controlled by a conformational transition in the protein (El-Sayed, 1993) that affects electrostatic interaction of these residues and their hydrogen bonding with surrounding charged and polar groups and water molecules (Rothschild, 1992; Maeda, 1995; Lanyi, 1998). This network of hydrogen bonds is very sensitive to the mutation of residues in the retinal binding pocket and in the proton channels connecting the Schiff base with the extracellular and cytoplasmic surfaces. Some mutations result in severe alterations of the photocycle and of the proton pumping activity of bR (Subramaniam et al., 1991; Otto et al., 1990; Needleman et al., 1991; Sonar et al., 1993; Balashov et al., 1993; Govindjee et al., 1995; Lanyi and Váró, 1995).

Arg^{82}, together with Asp^{85}, Asp^{212}, and water molecules, forms a complex counterion to the protonated Schiff base (De Groot et al., 1989). Replacement of a positively charged Arg^{82} with a neutral residue, glutamine or alanine, results in a dramatic increase in the pK_a of Asp^{85}, by 4.6 units from 2.6 to ~7.2 (Otto et al., 1989; Subramaniam et al., 1990; Balashov et al., 1993; Brown et al., 1993), and correspondingly, an increase in the pK_a of the purple-to-blue transition, which is associated with the protonation of Asp^{85} (Subramaniam et al., 1990; Metz et al., 1992). The rate of M formation is very fast in these mutants, indicating that the elevated pK_a of Asp^{85} in the unphotolyzed state facilitates light-induced Schiff base deprotonation and M formation (Balashov et al., 1995). At the same time, the light-induced proton release is delayed until the end of the photocycle (Balashov et al., 1993; Brown et al., 1995a; Otto et al., 1990), indicating that Arg^{82} is part of the mechanism for fast proton release (Govindjee et al., 1996). Motion of Arg^{82} may be involved in this process (Balashov et al., 1993; Scharnagl et al., 1995; Dickopf and Heyn, 1997). Perturbation of Arg^{82} was detected upon M formation (Petkova et al., 1999). Substitution of Arg^{82} for lysine partially restores the fast proton release; however, the coupling between Asp^{85} and the proton release group in R82K is not as strong as in the WT. The pK_a of Asp^{85} is 4.5 in the R82K mutant (versus 2.6 in WT). This indicates that although positive charge is important for the residue in the 82 position, the unique hydrogen bonding capabilities of the guanidinium group are also an important factor in tuning and coupling of the pK_a's of Asp^{85} and the proton release group. The conservative R82K mutation helped to reveal the complex titration of Asp^{85} due to coupling of Asp^{85} with the proton release group (Balashov et al., 1995). This important feature was also later demonstrated for the wild-type protein (Balashov et al., 1996).

In this report we investigated the consequences of the substitution of Arg^{82} with a potentially positively charged residue, histidine. The location of Arg^{82} in bR and several key residues involved in the proton transport in the extracellular channel based on the coordinates of Luecke et al.

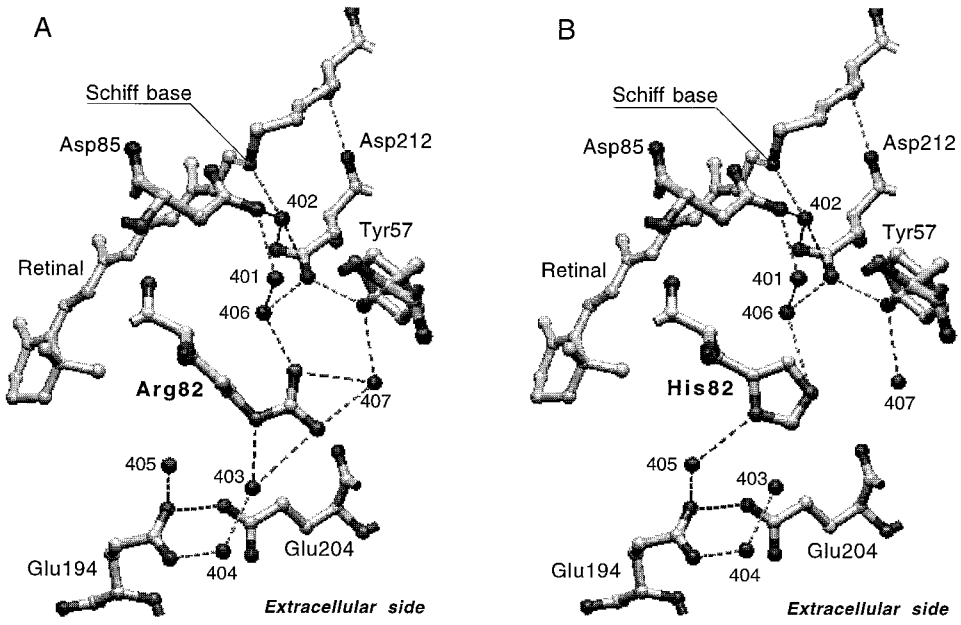

FIGURE 1 (*A*) The location of Arg^{82}, other key residues involved in the proton transport in the extracellular channel of bR based on the coordinates of Luecke et al. (1999). (*B*) Replacement of Arg^{82} with histidine, using utilities of Swiss-PdbViewer to illustrate the possible position of His^{82} in the R82H mutant. Dashed lines represent possible hydrogen bonds.

(1999) are shown in Fig. 1 *A*. The side chain of Arg^{82} is connected to the Schiff base, Asp^{85}, Asp^{212}, and the Glu^{194}–Glu^{204} site by a hydrogen bonded network involving several water molecules. The replacement of Arg^{82} with histidine, simulated in Fig. 1 *B*, might result in changes of hydrogen bonding of residue 82 with water molecules and in perturbation of the environment of Asp^{212}, Asp^{85}, Glu^{204}, and Glu^{194}. We have found that the R82H mutation alters several features of the unphotolyzed pigment and its photocycle reactions, presumably by affecting hydrogen bonding and electrostatic interactions in the proton release channel. The pK_a of Asp^{85} is extremely low in the R82H mutant (1 versus 2.6 in the WT). The K $\rightarrow$ L, L $\rightarrow$ M, and O $\rightarrow$ bR transitions are strongly affected. The M intermediate is not observed at pH 3, although the pigment is purple and undergoes light-dark adaptation. The amount of M increases with two pK_a's ($\sim$4.5 and 9.4). The group with pK_a 4.5 is also seen in the pH dependence of dark adaptation. These data suggest that two distinct titrable groups control light-induced Schiff base deprotonation and proton affinity of Asp^{85} in the R82H mutant of bacteriorhodopsin.

MATERIALS AND METHODS

The construction and expression of the R82H mutant in *Halobacterium salinarum* was done as described for the R82A (Balashov et al., 1993) and R82K (Balashov et al., 1995) mutants. The absorption spectra were recorded on a Cary-Aviv 14DS spectrophotometer (Aviv Associates, Lakewood, NJ). The pH titration and dark adaptation experiments were performed as described in our earlier studies (Balashov et al., 1993, 1995, 1996). Titration of the purple-to-blue transition was done in dark-adapted samples. To prevent aggregation and sedimentation at low pH, the pigment suspension in a 1-cm cuvette was constantly stirred. Flash photolysis experiments were done as described previously (Govindjee et al., 1990; Balashov et al., 1991, 1993). The kinetic traces were fit to two exponential components, using the utilities of KaleidaGraph (Synergy Software). All measurements of photocycle kinetics were done at 20°C on light-adapted samples. The pH-sensitive dye pyranine, at a concentration of 25 μM, was used to measure the light-induced pH changes in suspensions of R82H pigment (concentration 16 μM). The pathlength of the cuvette was 5 mm. To obtain the light-induced absorption changes of the dye, the trace taken in the absence of the dye was subtracted from the trace taken in the presence of the dye. For experiments at low pH, acrylamide gels that prevent aggregation at low pH were used. Gels were prepared as described by Liu et al. (1991), except that the purple membrane orientation step was omitted. Gels were incubated at a given pH for at least 12 h. A mixture of six pH buffers (5 mM of citric acid, 2-(*N*-morpholino)ethanesulfonic acid, HEPES, 3-(*N*-morpholino)propanesulfonic acid, 2-(*N*-cyclohexylamino) ethanesulfonic acid, 3-[cyclohexylamino]-1-propanesulfonic acid) was used to stabilize the pH between 2 and 11 for the dark adaptation experiments. The optical density of the samples for flash-induced absorption changes measurements was 0.3–0.4.

RESULTS

Unusually low pK_a of the purple-to-blue transition in the R82H mutant

Decreasing the pH from 7 to 2 causes a shift in the absorption maximum from 552 to 605 nm in a dark-adapted suspension of WT (Fischer and Oesterhelt, 1979). This is the so-called purple-to-blue transition, which is associated with the protonation of Asp^{85} (Subramaniam et al., 1990; Metz et al., 1992). In R82H, decreasing the pH to 2 causes only a slight shift in the absorption maximum and the formation of a small amount of the blue membrane (Fig. 2 *A*). The major purple-to-blue transition occurs at unusually low pH: the absorption maximum shifts from 558 nm to 622 nm as the pH is decreased to 0.2 in 75 mM K_2SO_4. The pH dependence of the absorption changes at 660 nm reveals two transitions (Fig. 3, *curve 1*). The pK_a of the minor transition ($\sim$10% of the absorption change) is 3.0 ($n = 1$), whereas the pK_a of the major transition is 1.0 ($n = 2.5$), much lower than the pK_a in the WT (2.6) (Fig. 3, *curve 3*). The absorption changes are slightly different in the two transitions (Fig. 2 *B*). The minor transition with pK_a 3.0 is characterized by an isosbestic point at 600 nm, a maximum at 640 nm, and a minimum at 565 nm. The minimum in the difference spectrum at 565 nm indicates that presumably all-*trans* pigment undergoes this transition because the 13-*cis* pigment absorbs at shorter wavelengths in WT and in R82H. The difference spectra of the second transition have their isosbestic point at 590 nm, their minimum at 542 nm, and their maximum at 640 nm.

Titration in the presence of 150 mM KCl shows formation of much less blue membrane than in the presence of 75 mM K_2SO_4, but with approximately the same pK_a (Fig. 3, *curve 2*). The decrease in the fraction of the blue membrane in the presence of KCl at low pH is caused by the transformation of the pigment into the acid purple species upon chloride binding to the blue membrane (Fischer and Oesterhelt, 1979; Kelemen et al., 1999). In the R82H mutant the chloride effect is stronger than in the WT at the same pH. We estimate that at pH 0.1 the chloride binding constant is 10 mM in R82H, whereas it is 100 mM in the WT (Váró and Lanyi, 1989; Renthal et al., 1990).

Spectral transitions in R82H at high pH

The WT pigment undergoes two pH-dependent transitions at high pH: transformation into an alkaline form accompanied by small red shifts of the chromophore (Balashov et al., 1991; Maeda et al., 1986) and tryptophan (Balashov et al., 1991) absorption bands, and the transformation into a P480 species (Druckmann et al., 1982; Balashov et al., 1991). These transitions are indicative of the deprotonation of the proton release group in the initial state of the protein and may be used to determine the pK_a of this group (Balashov et al., 1995; Govindjee et al., 1997). Similar transitions were observed in the R82H mutant.

Red shift of the chromophore and tryptophan absorption bands

Increasing the pH from 7.4 to 10.7 causes a small (2 nm) red shift in the absorption maximum of dark-adapted R82H membranes, from 558 nm to 560 nm (Fig. 4 *A*). The difference spectrum has its absorption maximum at 612 nm, isosbestic point around 572 nm, and minimum at 540 nm.

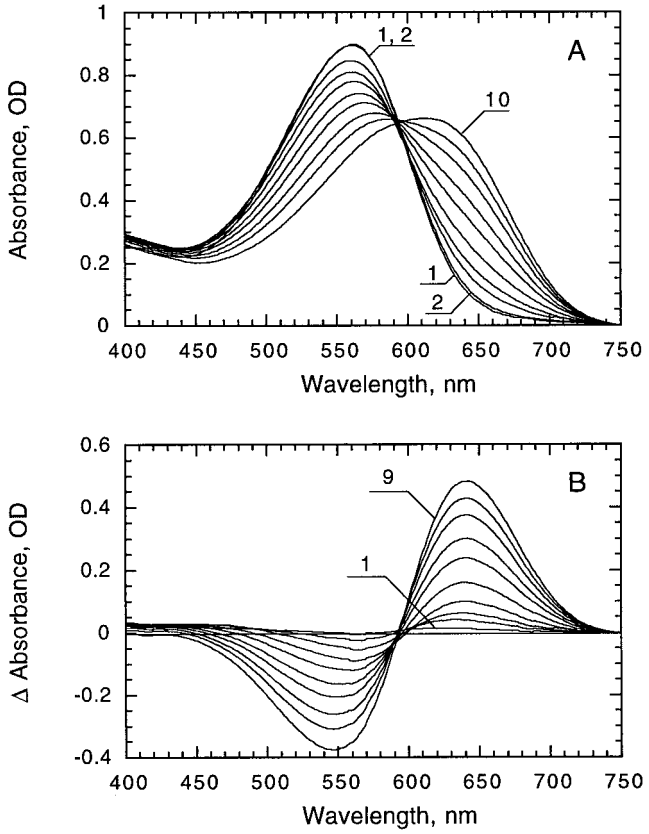

FIGURE 2 (*A*) Absorption spectra of the R82H mutant as the pH is decreased from 6.8 to 0.5 in 75 mM K_2SO_4. Spectra 1–10 were measured at pH 6.8, 3.3, 2.1, 1.5, 1.3, 1.1, 0.9, 0.8, 0.6, and 0.5, respectively. (*B*) Difference absorption spectra 1–9 were obtained as a difference between spectra taken at pH_i (given in *A*) and at pH 6.8.

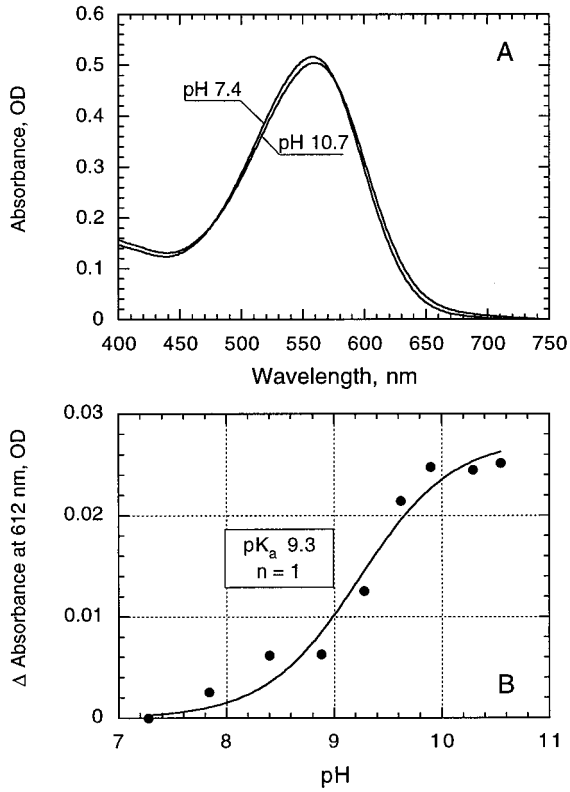

FIGURE 4 Spectral shift of the chromophore absorption band of the R82H mutant at high pH. (*A*) Red shift of the absorption spectrum of dark-adapted R82H as the pH is increased from 7.4 to 10.7. (*B*) pH dependence of absorption changes at 612 nm due to a red shift of the chromophore absorption band.

The pH dependence of the absorbance increase at 612 nm has a pK_a of 9.3 ± 0.1 (Fig. 4 *B*). In light-adapted R82H, the absorption maximum shifts 4 nm, from 568 nm at pH 6.8 to 572 nm at pH 10.7. The pH dependence of absorption changes at 612 nm in light-adapted pigment has a pK_a of 9.4 ± 0.1.

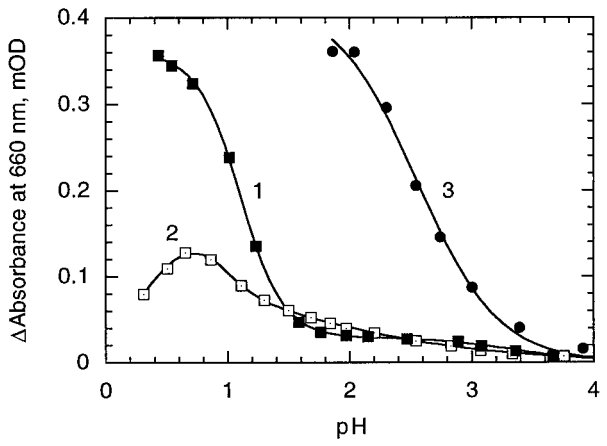

FIGURE 3 The pH dependence of the absorption changes at 660 nm due to the purple-to-blue transition in *1*, R82H mutant in 75 mM K_2SO_4; *2*, R82H mutant in 150 mM KCl; *3*, WT in 75 mM K_2SO_4.

In the UV, a small red shift of the tryptophan absorption band is observed as the pH is increased. To reveal these small absorption changes we used second derivatives of the pH-induced difference spectra (Fig. 5 *A*). The amplitude in the second derivative spectrum is inversely proportional to the square of the half-width of the absorption band, so the small but sharp tryptophan bands are enhanced in the second derivative spectrum. The pK_a of the tryptophan absorption band shift in R82H (determined from the amplitude at 285 nm in the second derivative spectra) is 9.4 ± 0.1 (Fig. 5 *B*), the same as that for the chromophore absorption shift (Fig. 4 *B*). It should be mentioned that the amplitudes of the absorption changes in the tryptophan absorption bands are half of those of the wild type under similar conditions (data not shown).

Formation of P480 species

At pH above 10.5 transformation of the pigment into a blue-shifted species absorbing at 480 nm takes place, and above pH 12.2 deprotonation of the Schiff base occurs. In R82H, P480 appears only at very high pH, whereas in the WT, R82Q, and K129H mutants a significant fraction of the

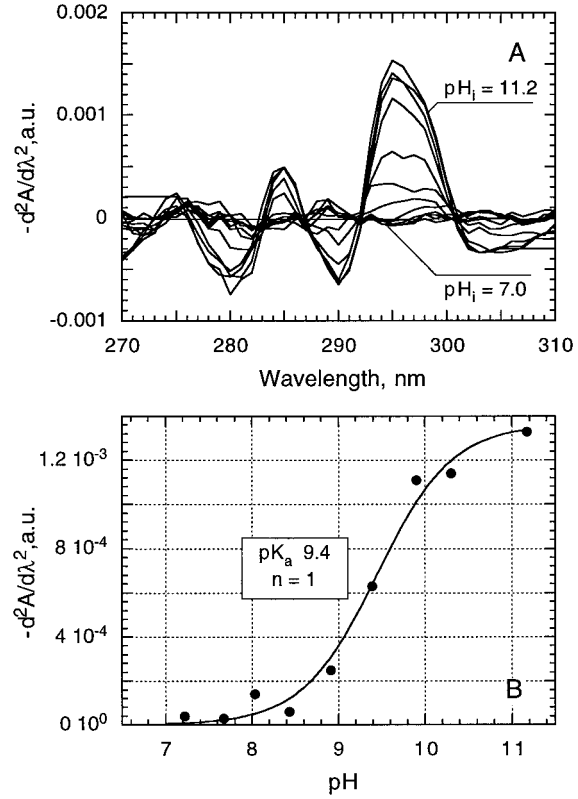

FIGURE 5 (*A*) Second derivatives of the difference absorption spectra in the UV as the pH is increased from 7.0 to 11.2. The change at 285 nm is due to the perturbation of a tryptophan residue. (*B*) The pH dependence of the amplitude of the second derivative (measured as a difference between 285 and 280 nm).

pigment converts into P480 already at pH 9 (Balashov et al., 1991; Govindjee et al., 1997).

Light adaptation of R82H

Light adaptation (13-*cis*-15-*syn* → all-*trans* photoisomerization of the chromophore) in R82H produced by blue light at the pH range between 3 and 9 causes a shift of the absorption maximum from 558 nm to 568 nm and an increase of absorbance at the maximum (Fig. 6) similar to that in the WT. At high pH (10.5), the difference spectrum of light adaptation is slightly shifted to longer wavelengths (because of the chromophore absorption shift) but has the same amplitude. The latter is different from the R82K mutant, in which light adaptation produces more all-*trans* species at high pH compared to neutral pH because of the pH-dependent photoreversibility of light adaptation at neutral pH (Balashov et al., 1995). In R82H light adaptation is also partially photoreversible. This results in the presence of some fraction of 13-*cis*-pigment even in the light-adapted membranes, particularly upon red light illumination. Illumination of a suspension of R82H with red light (>600 nm) that is absorbed mainly by the all-*trans* pigment partially reverses changes produced by blue-light illumination, transforming part of all-*trans* pigment into 13-*cis* (Fig. 6, *curve 3*). In R82H the yield of 13-*cis* pigment is not large, and unlike in R82K it does not show a pH dependence.

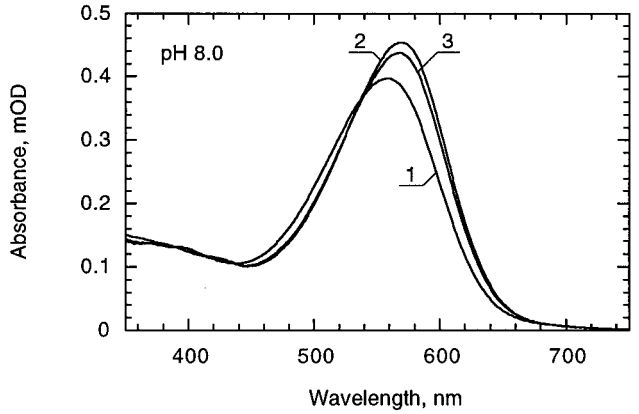

FIGURE 6 Light adaptation of the R82H mutant at pH 8.0: *1*, dark-adapted sample; *2*, after illumination with blue light (500–580 nm); *3*, after subsequent illumination with orange light (580–600 nm).

pH dependence of dark adaptation of R82H

As we showed earlier, at a given pH the rate constant of dark adaptation, k_{da}, is proportional to the fraction of blue membrane, f_{bm}, in the WT (Balashov et al., 1996), R82A (Balashov et al., 1993), R82K (Balashov et al., 1995), and other mutants (Govindjee et al., 1997; Balashov et al., 1997, 1999). Because of the coupling between the pK_a of Asp^{85} and the proton release group, analysis of the pH dependence of dark adaptation (and thus the protonation state of Asp^{85}) enables us to determine the pK_a of the proton release group. We apply this approach to the study of the interaction of Asp^{85} with ionizable groups in the R82H mutant.

The absorption changes upon dark adaptation in R82H at neutral pH are similar to those in the WT. However, the rate of dark adaptation is much slower. The time constant is 90 h at 20°C for pH 7.0 (versus 3 h in the WT at the same pH; see Fig. 7). The pH dependence of the rate constant of dark adaptation is different from that of the WT. It shows two pK_a's (1 and 4.5) and a plateau between pH 6 and 10 (Fig. 7, *curve 1*). The transition seen in WT with pK_a around 9 (Fig. 7, *curve 2*) is absent (or hidden) in R82H. From the pH dependence of k_{da} it follows that a group with a pK_a of 4.5 affects the proton affinity of Asp^{85} in R82H. Deprotonation of this group results in an increase in the pK_a of Asp^{85}, which correlates with an increase in the amount of the M intermediate (see below).

Two ionizable groups with pK_a 4.5 and 9.4 control formation of the M intermediate in R82H

Fig. 8 *A* depicts the flash-induced absorption changes at 410 nm caused by formation of the M intermediate at different pHs. Almost no M is accumulated at pH 3, although most of the pigment is in the purple (unprotonated Asp^{85}) form. As

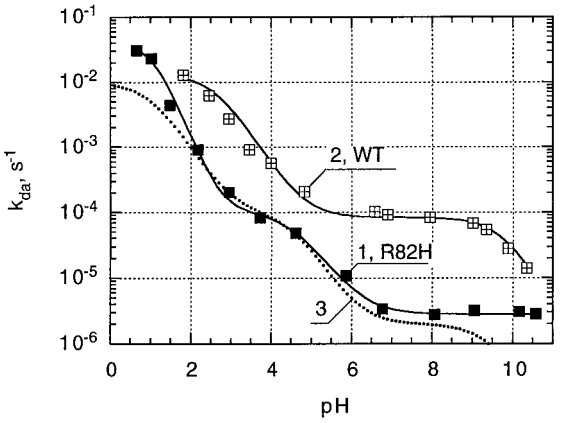

FIGURE 7 pH dependence of the rate constant of dark adaptation. *1*, R82H mutant; *2*, WT from Balashov et al., (1996), 20°C, 75 mM K_2SO_4; *3*, analytical curve for the fraction of blue membrane multiplied by k°_{da} = 0.01 to normalize with the slow component of k_{da} (Balashov et al., 1996). For a detailed description see the Discussion and the legend to Fig. 13.

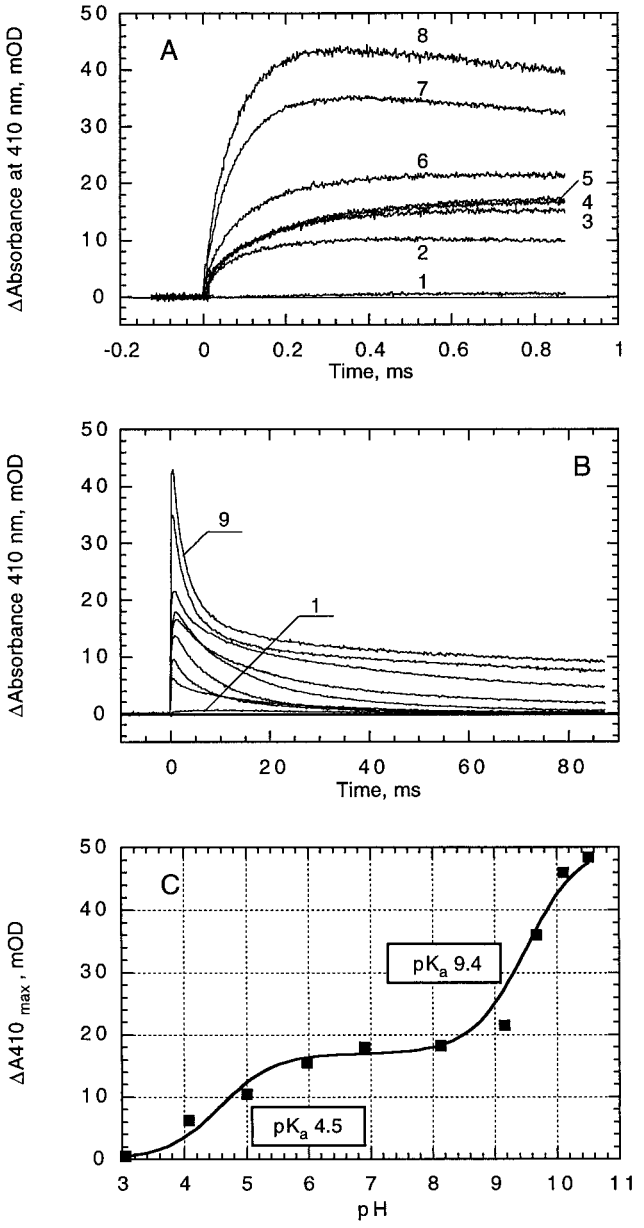

FIGURE 8 (*A*) Kinetics of M formation at pH 3.0, 5.0, 6.0, 6.9, 8.1, 9.2, 9.7, 10.0 (*curves 1–8*, respectively). (*B*) Kinetics of M decay at pH 3.0, 4.1, 5.0, 6.0, 6.9, 8.1, 9.2, 9.7, 10.0 (*curves 1–9*, respectively). (*C*) The pH dependence of the maximum light-induced absorption changes at 410 nm.

the pH is increased from 3 to 6 the amount of M gradually increases with a pK_a of 4.5. Between pH 6 and 8 the yield of M does not change substantially. Increasing the pH from 8 to 10 results in the 2.5-fold further increase in the yield of M (Fig. 8, *A* and *B*). The pK_a of this increase is 9.4. These results are different from those for the WT, where the amount of M does not change between 7 and 10. At low pH, first a small decrease (15–20%) in the maximum fraction of M in the WT is observed with pK_a 5.8 because of the shift in the L ↔ M equilibrium toward L (Zimányi et al., 1992). The major decrease in the fraction of M in the WT is at pK_a ~3 (in 150 mM salt) and coincides approximately with the pK_a of the purple-to-blue transition.

The kinetics of the light-induced Schiff base deprotonation (the L-to-M transition) are slower in R82H than in the WT. Between pH 6 and 8, the M intermediate formation kinetics can be approximated with a 140-μs time constant (versus 80 μs in WT; Liu, 1990). A better fit of the kinetics of M formation can be obtained with two components: τ_1 = 61 μs (34%) and τ_2 = 200 μs (66%), which are analogous to the two major components in the M formation for the WT, 35 μs (36%) and 144 μs (64%) at pH 7 (Heberle et al., 1993; Cao et al., 1995). Between pH 8.5 and 10.5 the rate constant of M formation increases in R82H, which perhaps explains the increase in the fraction of M (Fig. 8). At pH 10.5, M is formed with time constant τ = 50 μs (using a one-component fit), 2.7 times faster than at pH 7. In a two-component fit, τ_1 = 20 μs (30%) and τ_2 = 75 μs (70%); both components are accelerated by a factor of ~3 at pH 10.5 as compared to neutral pH. However, this is still much slower than for WT at high pH, where the formation of M occurs with 0.3-μs and 6-μs components (Liu, 1990). In R82H at pH 3, where a very small amount of M is formed, the rise time of M shows two components of approximately equal amplitude, 250 μs and 4–5 ms.

The ratio of the absorbance changes at 410 and 580 nm is pH dependent in R82H. The bleaching signal at 580 nm consists of an initial unresolved decrease in absorbance, caused mainly by the bR → L transition, and a slower component that coincides with the M formation (Fig. 8). The light-induced decrease of absorbance at 580 nm 1 ms after the flash is about the same at pH 6.8 and 10 (Fig. 9, *A* and *B*), whereas the amount of M formed is 2.5 times greater at pH 10 than at pH 6.8. The ratio of absorbance at 410 nm and 580 nm is 0.3 at pH 6.8 and 0.5 at pH 10 in the R82H mutant. In the WT, this ratio is ~0.5 at both high and neutral pH. Thus at high pH, the yield (maximum fraction) of M in R82H is similar to that in the WT but is decreased at neutral pH.

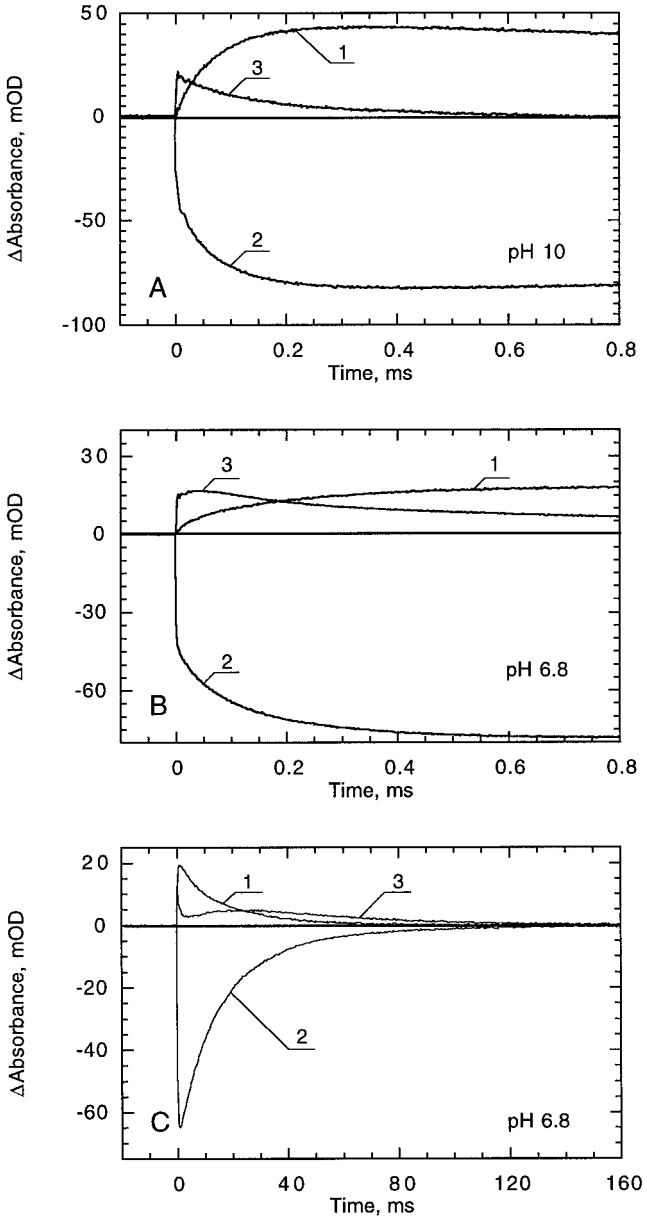

FIGURE 9 Kinetics of the flash-induced absorption changes in the R82H mutant: at 410 nm (*1*), 580 nm (*2*), and 660 nm (*3*). (*A*) pH 10.0; (*B*) pH 6.8; (*C*) pH 6.8 (longer time scale).

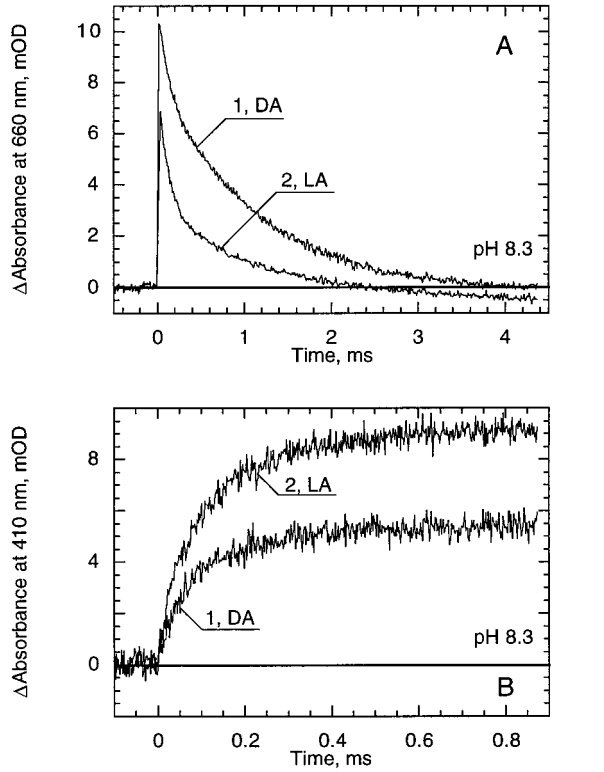

FIGURE 10 Effect of light adaptation on the amplitude and kinetics of the flash-induced absorption changes in the R82H mutant at 660 nm and 410 nm at pH 8.3. *1*, Dark-adapted (DA) sample; *2*, light-adapted (LA) sample. (*A*) 660 nm. The traces can be fit with two components: *1*, DA: 120 μs (2.6 mOD); 1.2 ms (8.8 mOD). *2*, LA: 120 μs (5.0 mOD), 1.2 ms (3.5 mOD). (*B*) 410 nm. The kinetics of M rise in DA and LA samples can be fit with two components, 40 μs and ~200 μs, with approximately equal amplitudes.

Decay of bathoproducts in light-adapted and dark-adapted R82H: the bathoproduct of the all-*trans* pigment has a long-lived component

A fast (unresolved) light-induced absorbance increase at 660 nm is observed in light-adapted R82H at all pHs. At pH range 6–8.5 it decays with two components of ~120–150 μs (45%) and ~1.2 ms (55%) (Fig. 10 *A*). The faster component correlates with the kinetics of M rise both at pH 8.3 (compare Fig. 10, *A* and *B*) and at pH 10 (Fig. 9 *A*) and can be assigned to the decay of the bathoproduct K of the all-*trans* pigment. In the WT, K decays much faster, in ~1–2 μs (Lozier et al., 1975; Váró and Lanyi, 1991; Chizhov et al., 1996). The amplitude of the 150-μs component is two times smaller in the dark-adapted sample, whereas the amplitude of the 1.2-ms component increases upon dark adaptation (Fig. 10 *A*). This indicates that the slower (1.2 ms) transition is associated with the 13-*cis* pigment. In the dark-adapted WT, an analogous photoproduct has a much slower decay time, 37 ms (Sperling et al., 1977; Balashov et al., 1993). However, in the R82A and R82K mutants, the decay of the analogous photoproduct is also very fast: 1 ms and 0.2 ms, respectively (Balashov et al., 1993, 1995).

The equilibrium in the K ⇔ L transition is shifted to K in R82H

The light-induced absorption changes measured 1 μs after the flash in light-adapted R82H at pH 6.8 show a positive band at 640 nm caused by formation of the bathoproducts of all-*trans*- and 13-*cis*-bR (Fig. 11 *A*, *curve 1*). The spectrum indicates that a significant amount of the K intermediate is not converted into L before M formation, and that the K ⇔ L equilibrium is shifted to K. This is different from the WT, in which the positive band is practically absent in light-adapted samples at neutral pH because of the almost com-

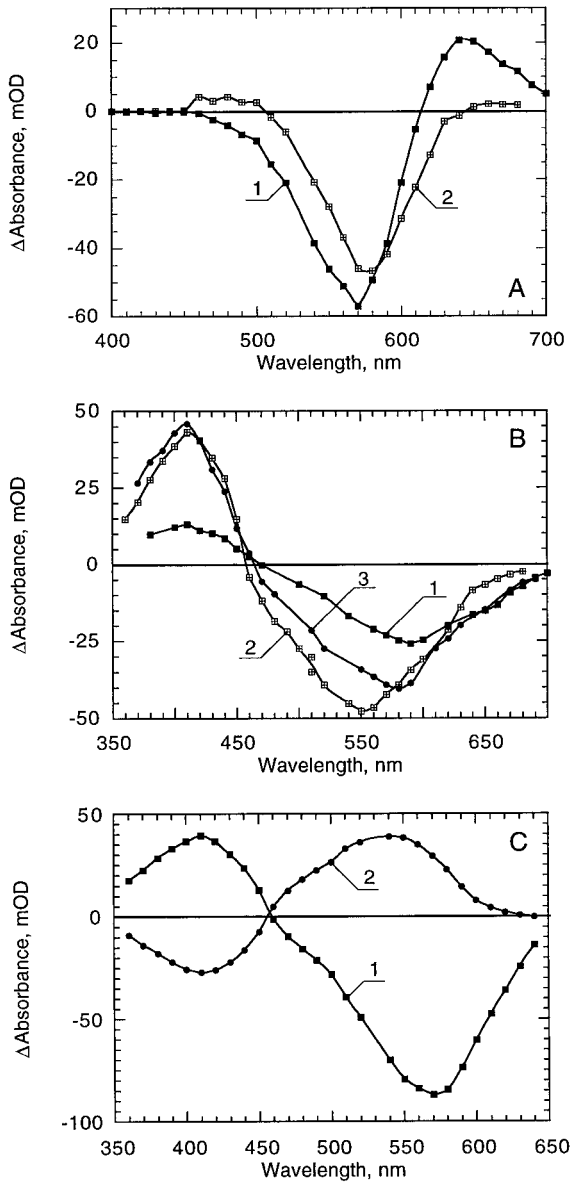

FIGURE 11 Light-induced difference absorption spectra of (*A*) BR → K → L transformations measured 1 μs after a flash in R82H (*1*) and WT (*2*). (*B*) Difference spectra of M formation: *1*, in R82H at pH 6.8; *2*, in WT at pH 6.8; *3*, in R82H at pH 10. Spectra 1 and 3 were obtained by plotting the amplitudes of the 200-μs and 75-μs components of the light-induced absorption changes (that coincide with M rise), respectively. Spectrum 2 is the difference between spectra taken 1 ms and 1 μs after the flash. (*C*) Light-induced difference spectra in R82H at pH 10 caused by *1*, transformation of initial R82H into M, obtained as the absorption changes measured 0.5 ms after the flash; *2*, transformation of M into N, obtained as a plot of the amplitude of the 2.5-ms component of the light-induced absorption changes.

plete transformation of the K intermediate into L within 1 μs after the flash (Fig. 11 *A*, *curve 2*). The difference spectra of M formation (Fig. 11 *B*) provide further evidence that the fraction of L intermediate is decreased in R82H. The spectrum at pH 6.8 (Fig. 11 *B*, *curve 1*) shows a negative band at 590 nm caused by transformation of the bathoproduct K. In the WT the minimum of the negative band is at 550 nm (close to the peak of the L intermediate), and the amount of the M photoproduct is more than twice as much as in R82H (Fig. 11 *B*, *curve 2*). At pH 10 (Fig. 11 *B*, *curve 3*) a larger amount of M formed than at pH 6.8. The minimum in the difference spectrum is at 580 nm. It indicates that the K ⇔ L equilibrium is shifted to K in R82H, even at high pH.

The decay of the M intermediate and recovery of initial pigment is slowed, and the N intermediate is perturbed in R82H

At pH 6.8 M decay (Fig. 9 *C*) can be fitted with two components, 5 ms (35%) and 21 ms (65%). The recovery of initial pigment proceeds with 15-ms (84%) and 42-ms (16%) time constants. The first process with the 15-ms apparent time constant most likely includes 5-ms and 21-ms components that are resolved in the M decay; however, it is not entirely composed of them, because it has a much bigger amplitude. The second (42 ms) time constant of bR recovery measured at 580 nm coincides with the apparent time constant of the O-to-bR transition measured at 660 nm, which is slowed compared to that of the WT and becomes the rate limiting. The apparent constant of O rise (N → O transition) is 12 ms at pH 6.8. At pH 10 the fast component of M decay due to the M-to-N transition has a lifetime of 2.5 ms. By plotting the amplitude of the 2.5-ms component at different wavelengths we obtained the "N minus M" difference spectrum (Fig. 11 *C*). The absorption maximum of the N intermediate in R82H (540 nm) is substantially blue shifted compared to the WT (562 nm).

Light-induced proton release and uptake in R82H: pH dependence and correlation with photocycle reactions

Light-induced proton release and uptake in suspensions of R82H were monitored using the pH sensitive dye pyranine. An increase in the dye absorbance at 462 nm reflects proton uptake by bR, while a decrease in absorbance is due to proton release into the medium (Heberle et al., 1994). In the R82H mutant the shape of the transient dye signal is pH dependent around neutral pH (Fig. 12 *A*). At pH 7.3 light-induced proton release has a time constant of 2 ms. It is followed by a 21-ms proton uptake phase, and then a slow, 49-ms component of proton release occurs (Fig. 12 *A*, *curve 1*). At lower pH (6.8) (Fig. 12 *A*, *curve 2*) the fraction of "fast" (2 ms) proton release decreases, whereas the amplitude of slow proton release increases. To estimate the fractions of "fast" and "slow" proton release, the pyranine traces were fitted with three components: fast proton release, proton uptake, and slow proton release, assuming that the sum of the fast and slow proton release components is equal to the proton uptake component (Govindjee et al., 1996). At pH 7.3 the fraction of fast (2 ms) proton release is 56%, whereas at pH 6.8 it is only 17%. At this pH most of the protons are released at the end of the photocycle. As shown

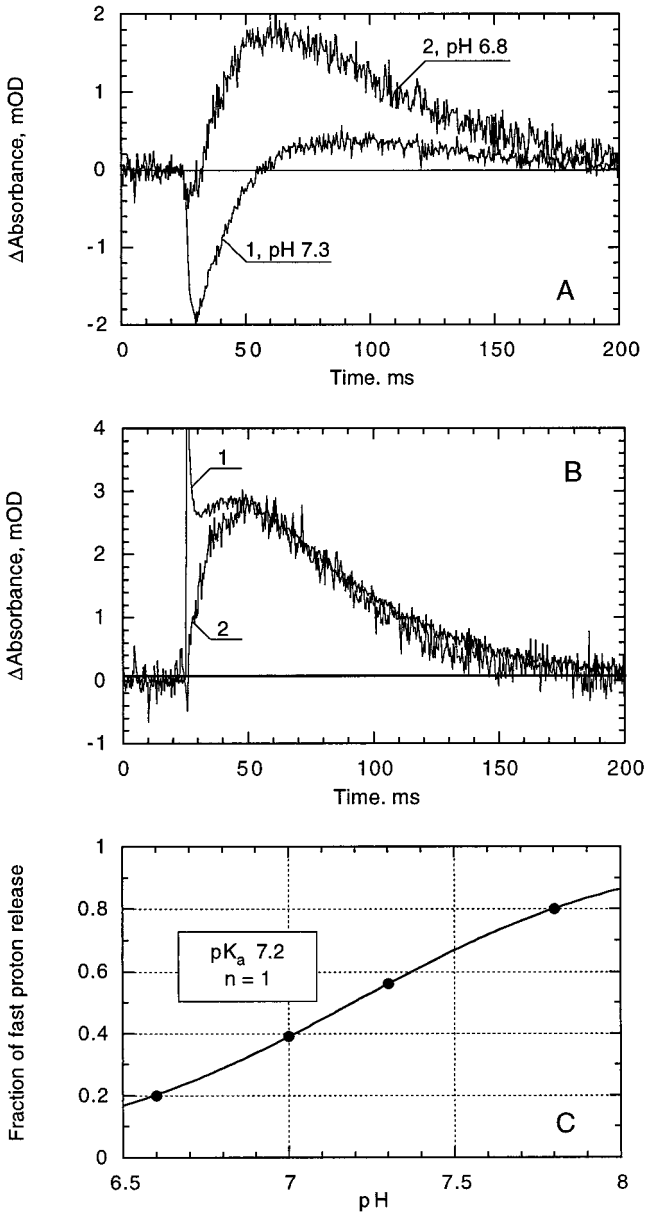

FIGURE 12 Light-induced proton release and uptake in R82H measured with pyranine (25 μM). (*A*) Light-induced absorbance changes of pyranine at 462 nm (obtained as a difference between traces with and without dye): *1*, at pH 7.3; *2*, at pH 6.8. (*B*) Kinetics of *1*, absorption changes at 660 nm reflecting O formation and O decay at pH 6.6; *2*, the pyranine signal at the same pH. (*C*) pH dependence of the fraction of fast proton release.

in Fig. 12 *B*, slow proton release coincides with O decay. The O decay involves deprotonation of Asp^{85} (Hessling et al., 1993), transfer of the proton to the proton release group (Kandori et al., 1997; Balashov et al., 1999), and reestablishing the Asp^{85}-Schiff base interaction, together with relaxation of the chromophore and the protein (Zscherp and Heberle, 1997). The O $\rightarrow$ bR transition is greatly slowed in the R82H mutant compared to the WT (42 ms versus 1–3 ms at neutral pH in the WT; Ames and Mathies, 1990; Chizhov et al., 1996; Balashov et al., 1999), indicating that proton transfer from Asp^{85} to the proton release group is slowed in R82H by more than 15 times.

The fraction of fast proton release versus pH is plotted in Fig. 12 *C*. It increases with pK_a 7.2 in R82H mutant (compared to 5.8 in WT). This implies that the pK_a of the proton release group is ~7.2 in the proton-releasing state (M and possibly N; see Discussion) for the R82H mutant.

DISCUSSION

Very low pK_a of Asp^{85} in R82H

From the pH dependence of the purple-to-blue transition (Fig. 3) it follows that the pK_a of Asp^{85} is very low in R82H (1 versus 2.6 in the WT). This may be due to a stronger interaction of the positive charge of the histidine with the negative charge of Asp^{85} in the mutant due to a lesser delocalization of a positive charge on histidine as compared to arginine. Another possible factor is stronger interaction of Asp^{85} with the internal water molecules, whose positions can also be altered by mutation. Two–three waters are in the vicinity of Asp^{85} (Maeda, 1995; Fischer et al., 1994; Luecke et al., 1999). Our recent Fourier transform infrared data indicate that more water molecules interact with Asp^{85} in the R82H mutant than in WT (Maeda et al., unpublished result). Stronger hydration of Asp^{85} should result in stabilization of the ionized form of Asp^{85} (and so in a reduction of its pK_a). Finally, because the pK_a of Asp^{85} reflects its equilibrium with the extracellular side of the membrane, a change in the accessibility of Asp^{85} would also affect the pK_a. If "internal" interactions (interactions of Asp^{85} with the Schiff base, Asp^{212}, His^{82}, and water molecules) are the determining factor that sets the low initial (unphotolyzed) state pK_a of Asp^{85} in the R82H mutant, then one would expect that the unusually low pK_a of Asp^{85} will result in delayed Schiff base deprotonation or even a decreased fraction of the deprotonated Schiff base (M intermediate) in R82H, because of the relationship that the lower the pK_a of Asp^{85} the slower the light-induced deprotonation of the Schiff base (Balashov et al., 1995; Govindjee et al., 1995). This is exactly what is observed in the R82H mutant and in the Y57N mutant, in which Asp^{85} also has very low pK_a (~1) and the M intermediate is not observed at neutral pH (Soppa et al., 1989; Govindjee et al., 1995). A low pK_a of Asp^{85} and lack of M accumulation were also observed for D212N/R82Q (Brown et al., 1995b), which may indicate that perturbation of interaction between Asp^{85} and Asp^{212} may contribute to the low pK_a of Asp^{85} and low fraction of M. We think that at least two groups (another carboxylic group and/or lipid group) are coupled with Asp^{85} and undergo titration with pK_a around 1, affecting the titration of Asp^{85} in R82H (because $n = 2.5$). Notably, in the R82A mutant $n = 1$ (no other groups besides Asp^{85} titrate with pK_a 7). In the WT, $n = 1.7$, which also indicates the presence of a group that is coupled with Asp^{85} and undergoes titration in the same pH range.

Chromophore and tryptophan absorption bands shift in R82H at high pH

As the pH is raised in the WT, a small 2-nm red shift of the chromophore absorption band occurs (Balashov et al., 1991). It is absent in R82A (Balashov et al., 1993), E204Q (Govindjee et al., 1996), and E194C (Balashov et al., 1997) mutants but present in R82K (Balashov et al., 1995) with a somewhat altered pK_a (8.0 versus 9.3 in WT). This shift was interpreted as an indication of the effect of the deprotonation of a residue, presumably the proton release group (Balashov et al., 1995), on the chromophore's absorption spectrum. The red shift is larger in R82H than in WT (4 nm versus 2 nm in the light-adapted states of the pigments; Fig. 4), but the pK_a of the shift is similar to that in the WT (both ~9.4), indicating that the pK_a of the group responsible for the shift is not affected by the R82H mutation.

The shift of the tryptophan absorption band occurs at a pK_a similar to that of the chromophore absorption shift (Fig. 5). It seems plausible that these effects are caused by the electrostatic interaction of an ionizable group with pK_a of 9.4 with the chromophore and with a tryptophan (Balashov et al., 1991) and/or are caused by changes in hydrogen bonding of polar groups and internal water molecules in response to the deprotonation of the proton release group. The large effect of deprotonation of the proton release group on the M yield and on the kinetics of the light-induced Schiff base deprotonation (Fig. 8) indicates that changes in the pK_a of Asp^{85} also take place. Thus we consider the small red shifts of the chromophore and tryptophan absorption bands as an indication of a change of electrostatic interactions and hydrogen bonding in the pigment in response to the deprotonation of the proton release group. It is somewhat surprising that although the R82K mutation causes a substantial decrease in the unphotolyzed state pK_a of the proton release group from 9.5–9.7 to 8.0 (Balashov et al., 1995), the R82H mutation does not substantially affect this pK_a in the unphotolyzed state (although it affects the pK_a in M; see below). This observation supports the conclusion that deprotonation of Arg^{82} is not responsible for the spectral and photochemical transitions with pK_a around 9.3–9.5 in the WT (Brown et al., 1993; Govindjee et al., 1996). The pK_a of histidine is 6 pK units lower than that of arginine (in water), so one would expect some decrease in the pK_a of the transitions that are directly controlled by Arg^{82} upon substitution for histidine, but this is not observed.

pH dependence of the rate constant of dark adaptation

Our earlier studies on R82A (Balashov et al., 1993), R82K (Balashov et al., 1995), and the WT (Balashov et al., 1996) showed that the rate constant of dark adaptation, k_{da}, is proportional to the fraction of the blue membrane, f_{bm}: $k_{da}(pH) = k^{\circ}_{da} f_{bm}(pH)$, where k°_{da} is the maximum rate constant observed at low pH when all of the pigment is transformed into the blue membrane. This relationship holds for over three orders of magnitude of f_{bm} and was shown to be valid for other mutants such as K129H (Govindjee et al., 1997), E194C (Balashov et al., 1997), E204D (Dioumaev et al., 1998), and E194D (Balashov et al., 1999). It was interpreted as an indication that thermal isomerization occurs upon transient protonation of Asp^{85} and formation of blue membrane (Balashov et al., 1993, 1996; Balashov, 1995). The rate constant of thermal isomerization is at least 10^3 times higher in the blue membrane than in the purple, presumably because the barrier for isomerization is lower in the blue membrane because of a greater delocalization of π-electrons and the removal of electrostatic interactions between Asp^{85} and the Schiff base upon protonation of Asp^{85} (Balashov et al., 1996). The proportionality between k_{da} and f_{bm} has enabled us to use the pH dependence of dark adaptation as a tool to investigate the interaction of the primary proton acceptor, Asp^{85}, with other ionizable residues—especially potential members of the proton release pathway. Because of the interaction of Asp^{85} with a group with pK_a of ~9.5–9.7, the titration curve of Asp^{85} is biphasic in the WT (Balashov et al., 1993, 1996).

In the R82H mutant the pH dependence of the rate constant of dark adaptation shows two pK_a's, 1 and 4.5 (Fig. 7). The first one coincides with the pK_a of the major component of the purple-to-blue transition (Fig. 3), which is in agreement with the proportionality between k_{da} and f_{bm}. The second component with pK_a 4.5 has not been observed before in the WT or other mutants. However, titration of the purple-to-blue transition and the pH dependence of dark adaptation in the E194D mutant do indicate that besides the group with a pK_a around 9, there is another group with a pK_a around 3 that is also coupled with Asp^{85}, but it has a significantly smaller coupling strength (Balashov et al., 1999). The fit of the pH dependence of k_{da} with our coupling model (Balashov et al., 1995, 1996) indicates that in R82H deprotonation of the group with pK_a 4.5 shifts the pK_a of Asp^{85} from 1 to 2.5. This increase in the proton affinity of Asp^{85} provides an explanation for the increase in the yield of M, which takes place with the same pK_a (Fig. 8). An alternative explanation of the pK_a 4.5 transition, that it is due to the deprotonation of His^{82} itself, seems less likely, because one would expect a larger shift in the pK_a of Asp^{85} if His^{82} were to be neutralized and a quite different phenotype. The expected phenotype would be close to that of the neutral position 82 mutants, R82A and R82Q (Otto et al., 1990; Balashov et al., 1993; Brown et al., 1995b; Govindjee et al., 1996), where the pK_a of Asp^{85} is increased to 7.5 in the initial state, M formation is very fast (less than 1 μs), and no fast proton release is observed. R82H does not show these features, so we assume that His^{82} does not deprotonate with pK_a 4.5.

Above pH 5 the rate constant of dark adaptation is very slow—30 times slower than in the WT at pH 7—and it does not change with pH (Fig. 7). A similar pH-independent rate was also observed in the E204Q mutant above pH 6 (Richter et al., 1996). This basal rate can be interpreted as the rate constant for thermal isomerization of the chromophore in

the purple membrane (i.e., in the state when Asp^{85} is deprotonated). The pH dependence of k_{da} in R82H can be described by the following equation, which includes the rate constant of isomerization in the purple state, k_{da}^{pm}:

$$k_{da}(pH) = k_{da}^{\circ} f_{bm}(pH) + k_{da}^{pm}, \quad (1)$$

where k_{da}° is the rate constant of isomerization in the blue membrane and can also be designated as k_{da}^{bm}. As follows from Fig. 7, k_{da}° is $\sim 10^4$ times larger than k_{da}^{pm} in R82H. This translates into a decrease in the activation energy barrier for thermal isomerization upon protonation of Asp^{85} of ~5 kcal/mol. A theoretical calculation gives a similar value, 7 kcal/mol (Logunov and Schulten, 1996).

In R82H the basal rate probably masks the rate change due to the interaction of Asp^{85} with the high pK_a group that is seen in the WT and most mutants. However, the red shift of the chromophore and tryptophan absorption bands (Fig. 4) and the pH dependence of the formation of M (Fig. 8) show that a residue with pK_a 9.4 is present in R82H, and it affects the pK_a of Asp^{85}. The model that accounts for the presence of two ionizable groups (with pK_a 4.5 and 9.4) is discussed below. The pH dependence of k_{da} calculated from this model is shown in Fig. 7 (*curve 3*). Above pH 6.5 $k_{da}^{\circ} f_{bm}$ is less than k_{da}^{pm} and does not contribute substantially to the pH dependence of k_{da}.

pH dependence of the yield of M formation

Almost no M intermediate is formed at pH 3 in R82H (Fig. 8 *A*). The amount of M increases with pK_a 4.5 and pK_a 9.4 (Fig. 8). The possibility that this is caused by an increase in the fraction of *trans*-bR can be rejected because the absorption maximum of the light-adapted pigment does not change between pH 3 and pH 7. The fraction of M depends on the relative pK_a's of the Schiff base and Asp^{85} in the L ⇔ M equilibrium (Lanyi, 1993; Balashov et al., 1995). We suggest that deprotonation of each of the two residues with pK_a 4.5 and pK_a 9.4 results in an increase in the pK_a of Asp^{85}, and as a consequence, there is an increase in the rate constant of the (K + L) → M transition. The kinetic curves in Fig. 8 *A* and the pH dependence of M in Fig. 8 *C* can be approximately simulated using a simplified model of the photocycle, L ⇔ M → BR, and equations derived for a similar model (Balashov et al., 1999), assuming that the rate constant of the L → M transition, $k_{L\to M}$, is ~1.5 times less than the rate constant of the reverse reaction, $k_{M\to L}$, at pH 7 ($k_{L\to M} = 2000\ s^{-1}$, $k_{M\to L} = 3000\ s^{-1}$) and that $k_{M\to L}$ increases at least five times as the pH is increased to 10 and decreases about 10 times as the pH is decreased to 3. This indicates that changes in the pK_a of Asp^{85} caused by reprotonation of groups with pK_a 4.5 and 9.5 translate into changes in the rate constant of the L → M transition and thus can account for the observed pH dependence of the fraction of M.

The R82H mutation affects not only the L → M transition but also the preceding K → L transition, as one can see from Fig. 11, *A* and *B*. Because both the K → L and L → M transitions involve substantial changes in hydrogen bonding of three internal water molecules (Maeda et al., 1992; Maeda, 1995; Hatanaka et al., 1996; Kandori et al., 1995), it is likely that the R82H mutation affects the interaction of Asp^{85} with water molecules. Our Fourier transform infrared data support this possibility (Maeda et al., unpublished). Furthermore, because deprotonation of residues with pK_a's of 4.5 and 9.4 increases the yield of M, it is likely that these residues belong to the same hydrogen-bonded network, most likely connecting Asp^{85} with the extracellular surface.

Proton release and uptake in R82H

Fig. 12 shows that the pK_a of fast proton release is 7.2 in the R82H mutant versus 5.8 in the WT (Zimányi et al., 1992). Thus the R82H mutation results in an increase in the pK_a of the proton release group in M of 1.4 pK units. This result supports the notion that Arg^{82} participates in the control of the pK_a of the proton release group (Balashov et al., 1993; Govindjee et al., 1996). However, in contrast to the R82K mutation, the pK_a of the proton release group is much less affected by R82H mutation in its unphotolyzed state than in M. As in E204Q (Brown et al., 1995a; Misra et al., 1997) and E194C (Balashov et al., 1997), slow proton release coincides with O decay (Fig. 12). Moreover, O decay is slowed compared to the WT, indicating a decrease in the rate of proton transport from Asp^{85} to the proton release group.

A model for describing the pH dependence of the proton affinity of Asp^{85}: implications for the pH dependencies of dark adaptation, M formation, and proton release in R82H

Previously we developed a model describing the coupling of the proton affinity (protonation state) of Asp^{85} with the protonation state of another residue X, which was identified as the proton release group in the pigment's unphotolyzed state (Balashov et al., 1995, 1996). The pH dependence of dark adaptation and, particularly, the pH dependence of M formation in R82H indicate that the deprotonation of two groups increases the pK_a of Asp^{85}: in addition to a high pK_a group X (pK_a 9.4), there is another group with pK_a 4.5 (we will call it Z). To accommodate this group and explain the pH dependencies of the rate constants of dark adaptation and M formation, we propose the following model, which couples the protonation state of Asp^{85} with the protonation states of both X and Z (Fig. 13). This expands our previous model of two interacting residues. The fraction of blue membrane in this model is described by the following equation:

$$f_{bm} = A/B, \quad \text{where } A = 1 + \alpha\beta; \quad B = A + (1 + \gamma\delta)\epsilon;$$
$$\alpha = 1 + 10^{(pH-pK_{a5})}; \quad \beta = 10^{(pH-pK_{a1})};$$
$$\gamma = 1 + 10^{(pH-pK_{a6})}; \quad \delta = 10^{(pH-pK_{a2})}; \quad \epsilon = 10^{(pH-pK_{a3})}. \quad (2)$$

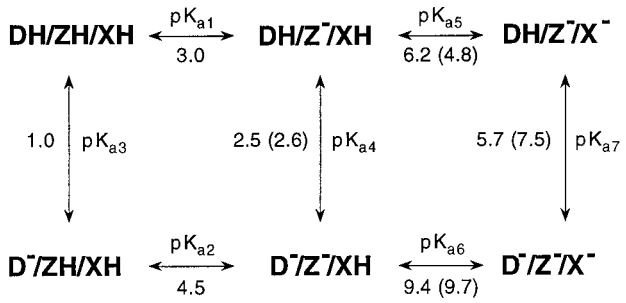

FIGURE 13 Model describing coupling of the pK_a of Asp^{85} with the protonation states of two residues, X and Z in R82H. D stands for Asp^{85}. Protonated states of D, X, and Z are designated as DH, XH, and ZH. Deprotonated states of D, X, and Z are designated as D^-, X^-, and Z^-. The model considers six different states of the unphotolyzed pigment that are engaged in pH-dependent equilibria. The pK_a values for R82H mutant were estimated from the titration of Asp^{85} (pK_{a3}) and the pH dependencies of dark adaptation (pK_{a1}, pK_{a2}, and pK_{a3}), the chromophore and tryptophan absorption shifts (pK_{a6}), M amplitude (pK_{a2} and pK_{a6}), and proton release (pK_{a5}), as described in the text. The fraction of blue membrane as a function of pH is calculated from this model using Eq. 2 and plotted in Fig. 7 (*curve 3*). The pK_a values for WT are given in parentheses. The pK_a values associated with residue Z in WT are not yet known. Most likely pK_{a2} is less than 2; in this case the experimentally determined pK_a of the purple-to-blue transition in the WT (2.6) corresponds to pK_{a4}.

Five pK_a's out of seven completely describe the equilibrium reactions shown in Fig. 13. The other two pK_a values can be determined from the relationships $pK_{a1} + pK_{a4} = pK_{a2} + pK_{a3}$ and $pK_{a4} + pK_{a6} = pK_{a5} + pK_{a7}$, which are expressions of the thermodynamics principle that the free energy difference in the equilibrium transitions between two states does not depend on the particular pathway traversed.

The pK_a's were estimated as described below. From the direct titration of the purple-to-blue transition and the pH dependence of dark adaptation, we conclude that the pK_a of Asp^{85} when both Z and X are protonated (pK_{a3}) is 1.0. From the pH dependence of dark adaptation (Fig. 7) and the pH dependence of the fraction of M (Fig. 8), it follows that the pK_a of Z when Asp^{85} is deprotonated (pK_{a2}) is equal to 4.5. Two other pK_a's related to Asp^{85} and the group Z that affects its proton affinity (pK_{a1} and pK_{a4}) can be determined from the pH dependence of dark adaptation (Balashov et al., 1995). It follows from the fit of k_{da} (Fig. 7) that the pK_a of Asp^{85} increases by ~1.5 units with the deprotonation of Z ($pK_{a4} = 2.5$), and correspondingly, the pK_a of Z also decreases by ~1.5 units with the protonation of Asp^{85} ($pK_{a1} = 3.0$). Thus the coupling strength (Balashov et al., 1999) of the interaction of Asp^{85} and Z is ~1.5.

Four processes take place in R82H with approximately the same pK_a of 9.4: the red shift of the chromophore absorption band, the red shift of the tryptophan band, the increase in the fraction of M, and the change in the rate of M formation. We attribute these changes to the deprotonation of the proton release group in the unphotolyzed state (Balashov et al., 1995) and assume that $pK_{a6} = 9.4$ in R82H. The pK_a of the fast component of proton release is 7.2. This pK_a characterizes the pK_a of the proton release group in M, where the Schiff base is deprotonated (Zimányi et al., 1992). In other mutants, its value is about one unit larger than the pK_a of this group in the blue membrane where the Schiff base is protonated (Balashov et al., 1995, 1996). From this we estimate that the $pK_{a5} = 6.2$ (7.2–1). Thus the coupling strength between Asp^{85} and the proton release group in R82H is 3.2. It is smaller than in the WT (4.8), but larger than in R82K (2.4).

Possible identification of the groups with pK_a's of 4.5 and 9.4

Our working hypothesis is that the group with pK_a 4.5 is not His^{82} itself but rather some residue in the proton release channel of bR. The most likely candidates are Asp^{212} and Glu^{194}. It has been shown that mutation of Asp^{212} to a neutral residue results in features that we observe in the R82H mutant—a low pK_a of Asp^{85} in D212N/R82Q mutant (Brown et al., 1995b) and a decreased amount of M, as also seen for the D212N mutant at pH < 7 (Needleman et al., 1991). It is possible that the R82H mutation causes an alteration in the hydrogen bonding of Asp^{212} (Fig. 1), which results in the increase in the pK_a of Asp^{212} from below 2 in the WT to ~4.5.

Alternative candidates for the group with pK_a 4.5 are Glu^{194} and other glutamic acid residues on the extracellular surface that affect the pK_a of Asp^{85}, Glu^{74} (Rodriguez et al., 1997), and Glu^{9} (our unpublished result). Glu^{194} is a key part of the proton release group (Balashov et al., 1997). According to Dioumaev et al. (1998), the pK_a of this group is low in the unphotolyzed state.

The origin of the pK_a 9.4 proton release group has been discussed in several recent papers (Balashov et al., 1995, 1996, 1997; Richter et al., 1996; Luecke et al., 1999; Dioumaev et al., 1998; Rammelsberg et al., 1998). There are several suggestions: that it is a water molecule between Arg^{82} and Glu^{204} (Luecke et al., 1999), that it is a complex of residues including Glu^{204} and Glu^{194} and water molecules associated with them (Balashov et al., 1997; Essen et al., 1998), and that it could be the whole network of hydrogen bonding residues in the extracellular channel, including Arg^{82}, Glu^{204}, and Glu^{194} (Rammelsberg et al., 1998). The fact that the R82H mutation did not substantially affect the pK_a of the proton release group in the unphotolyzed state shows that this group is not Arg^{82}. However, the decrease in the pK_a of the proton release group in M and dramatic slowdown of the O→bR transition and the rate of proton release at low pH go along with the notion that Arg^{82} controls the pKa of the proton release group and is crucial for efficient proton release from Asp^{85} to the surface.

CONCLUSION

The R82H mutant shows several features that are profoundly different from those of the WT. The most remarkable is the very low pK_a of the purple-to-blue transition

(pK_a of Asp^{85}), 1 versus 2.6 in the WT. The second finding is that protonation of a group with pK_a 4.5 that most likely is located in the extracellular proton release channel inhibits the light-induced proton transport from the Schiff base to Asp^{85} during formation of M, presumably by affecting the proton affinity of Asp^{85} through electrostatic interaction and/or alteration of hydrogen bonding. A model of three interacting residues is proposed to describe the effects of low pK_a (4.5) and high pK_a (9.4) groups on the proton transport. The O→bR transition is slowed in R82H indicating that Arg^{82} is important for the proton transfer from Asp^{85} to the proton release group.

This work was supported by National Institutes of Health grant GM52023 (to TGE), Department of Energy grant 95ER20171 (to RKC), and National Science Foundation grant EPS9630167.

REFERENCES

Ames, J. B., and R. A. Mathies. 1990. The role of back-reactions and proton uptake during the N → O transition in bacteriorhodopsin's photocycle: a kinetic resonance Raman study. *Biochemistry.* 29: 7181–7190.

Balashov, S. P. 1995. Photoreactions of the photointermediates of bacteriorhodopsin. *Isr. J. Chem.* 35:415–428.

Balashov, S. P., R. Govindjee, and T. G. Ebrey. 1991. Red shift of the purple membrane absorption band and the deprotonation of tyrosine residues at high pH. Origin of the parallel photocycles of trans-bacteriorhodopsin. *Biophys. J.* 60:475–490.

Balashov, S. P., R. Govindjee, E. S. Imasheva, S. Misra, T. G. Ebrey, Y. Feng, R. K. Crouch, and D. R. Menick. 1995. The two pK_a's of aspartate-85 and control of thermal isomerization and proton release in the arginine-82 to lysine mutant of bacteriorhodopsin. *Biochemistry.* 34:8820–8834.

Balashov, S. P., R. Govindjee, M. Kono, E. Imasheva, E. Lukashev, T. G. Ebrey, R. K. Crouch, D. R. Menick, and Y. Feng. 1993. Effect of the arginine-82 to alanine mutation in bacteriorhodopsin on dark adaptation, proton release, and the photochemical cycle. *Biochemistry.* 32: 10331–10343.

Balashov, S. P., E. S. Imasheva, T. G. Ebrey, N. Chen, D. R. Menick, and R. K. Crouch. 1997. Glutamate-194 to cysteine mutation inhibits fast light-induced proton release in bacteriorhodopsin. *Biochemistry.* 36: 8671–8676.

Balashov, S. P., E. S. Imasheva, R. Govindjee, and T. G. Ebrey. 1996. Titration of aspartate-85 in bacteriorhodopsin: what it says about chromophore isomerization and proton release. *Biophys. J.* 70:473–481.

Balashov, S. P., M. Lu, E. S. Imasheva, R. Govindjee, T. G. Ebrey, B. Othersen III, R. K. Crouch, and D. R. Menick. 1999. The proton release group of bacteriorhodopsin controls the rate of the final step of its photocycle at low pH. *Biochemistry.* 38:2026–2039.

Braiman, M. S., A. K. Dioumaev, and J. R. Lewis. 1996. A large photolysis-induced pK_a increase of the chromophore counterion in bacteriorhodopsin: implications for ion transport mechanisms of retinal proteins. *Biophys. J.* 70:939–947.

Brown, L. S., L. Bonet, R. Needleman, and J. K. Lanyi. 1993. Estimated acid dissociation constants of the Schiff base, Asp-85, and Arg-82 during the bacteriorhodopsin photocycle. *Biophys. J.* 65:124–130.

Brown, L. S., J. Sasaki, H. Kandori, A. Maeda, R. Needleman, and J. K. Lanyi. 1995a. Glutamic acid 204 is the terminal proton release group at the extracellular surface of bacteriorhodopsin. *J. Biol. Chem.* 270: 27122–27126.

Brown, L. S., G. Váró, M. Hatanaka, J. Sasaki, H. Kandori, A. Maeda, N. Friedman, M. Sheves, R. Needleman, and J. K. Lanyi. 1995b. The complex extracellular domain regulates the deprotonation and reprotonation of the retinal Schiff base during the bacteriorhodopsin photocycle. *Biochemistry.* 34:12903–12911.

Cao, Y., L. S. Brown, J. Sasaki, A. Maeda, R. Needleman, and J. K. Lanyi. 1995. Relationship of proton release at the extracellular surface to deprotonation of the Schiff base in the bacteriorhodopsin photocycle. *Biophys. J.* 68:1518–1530.

Chizhov, I., D. S. Chernavskii, M. Engelhard, K.-H. Mueller, B. V. Zubov, and B. Hess. 1996. Spectrally silent transitions in the bacteriorhodopsin photocycle. *Biophys. J.* 71:2329–2345.

De Groot, H. J. M., G. S. Harbison, J. Herzfeld, and R. G. Griffin. 1989. Nuclear magnetic resonance study of the Schiff base in bacteriorhodopsin: counterion effects on the ^{15}N shift anisotropy. *Biochemistry.* 28:3346–3353.

Dencher, N., and M. Wilms. 1975. Flash photometric experiments on the photochemical cycle of bacteriorhodopsin. *Biophys. Struct. Mech.* 1:259–271.

Dickopf, S., and M. Heyn. 1997. Evidence for the first phase of the reprotonation switch of bacteriorhodopsin from time-resolved photovoltage and flash photolysis experiments on the photoreversal of the M-intermediate. *Biophys. J.* 73:3171–3181.

Dioumaev, A., H.-T. Richter, L. S. Brown, M. Tanio, S. Tuzi, H. Saito, Y. Kimura, R. Needleman, and J. K. Lanyi. 1998. Existence of a proton transfer chain in bacteriorhodopsin: participation of Glu-194 in the release of protons to the extracellular surface. *Biochemistry.* 37: 2496–2506.

Druckmann, S., M. Ottolenghi, A. Pande, J. Pande, and R. H. Callender. 1982. Acid-base equilibrium of the Schiff base in bacteriorhodopsin. *Biochemistry.* 21:4953–4959.

Ebrey, T. G. 1993. Light energy transduction in bacteriorhodopsin. *In* Thermodynamics of Membrane Receptors and Channels. M. B. Jackson, editor. CRC Press, Boca Raton, FL. 353–387.

El-Sayed, M. 1993. On the molecular mechanisms of the solar to electric energy conversion by the other photosynthetic system in nature, bacteriorhodopsin. *J. Am. Chem. Soc.* 25:279–286.

Essen, L.-O., R. Siegert, W. D. Lehmann, and D. Oesterhelt. 1998. Lipid patches in membrane protein oligomeres: crystal structure of the bacteriorhodopsin-lipid complex. *Proc. Natl. Acad. Sci. USA.* 95: 11673–11678.

Fischer, U., and D. Oesterhelt. 1979. Chromophore equilibria in bacteriorhodopsin. *Biophys. J.* 28:211–230.

Fischer, W. B., S. Sonar, T. Marti, H. G. Khorana, and K. J. Rothschild. 1994. Detection of a water molecule in the active site of bacteriorhodopsin: hydrogen bonding changes during the primary photoreaction. *Biochemistry.* 33:12757–12762.

Gerwert, K., B. Hess, J. Soppa, and D. Oesterhelt. 1989. Role of aspartate-96 in proton translocation by bacteriorhodopsin. *Proc. Natl. Acad. Sci. USA.* 86:4943–4947.

Govindjee, R., S. P. Balashov, and T. G. Ebrey. 1990. Quantum efficiency of the photochemical cycle of bacteriorhodopsin. *Biophys. J.* 58: 597–608.

Govindjee, R., E. S. Imasheva, S. Misra, S. P. Balashov, T. G. Ebrey, N. Chen, D. R. Menick, and R. K. Crouch. 1997. Mutation of a surface residue, lysine-129, reverses the order of proton release and uptake in bacteriorhodopsin; guanidine hydrochloride restores it. *Biophys. J.* 72: 886–898.

Govindjee, R., M. Kono, S. P. Balashov, E. S. Imasheva, M. Sheves, and T. G. Ebrey. 1995. Effects of substitution of tyrosine 57 with asparagine and phenylalanine on the properties of bacteriorhodopsin. *Biochemistry.* 34:4828–4838.

Govindjee, R., S. Misra, S. P. Balashov, T. G. Ebrey, R. K. Crouch, and D. R. Menick. 1996. Arginine-82 regulates the pK_a of the group responsible for the light-driven proton release in bacteriorhodopsin. *Biophys. J.* 71:1011–1023.

Hatanaka, M., J. Sasaki, H. Kandori, T. G. Ebrey, R. Needleman, J. K. Lanyi, and A. Maeda. 1996. Effects of arginine-82 on the interactions of internal water molecules in bacteriorhodopsin. *Biochemistry.* 35: 6308–6312.

Heberle, J., and N. A. Dencher. 1992. Surface-bound optical probes monitor proton translocation and surface potential changes during the bacteriorhodopsin photocycle. *Proc. Natl. Acad. Sci. USA.* 89:5996–6000.

Heberle, J., D. Oesterhelt, and N. A. Dencher. 1993. Decoupling of photo- and proton cycle in the Asp85 → Glu mutant of bacteriorhodopsin. *EMBO J.* 12:3721–3727.

Heberle, J., J. Riesle, G. Thiedemann, D. Oesterhelt, and N. A. Dencher. 1994. Proton migration alone the membrane-surface and retarded surface to the bulk transfer. *Nature.* 370:379–382.

Hessling, B., G. Souvignier, and K. Gerwert. 1993. A model-independent approach to assigning bacteriorhodopsin's intramolecular reactions to photocycle intermediates. *Biophys. J.* 65:1929–1941.

Kandori, H., Y. Yamazaki, M. Hatanaka, R. Needleman, L. S. Brown, H.-T. Richter, J. K. Lanyi, and A. Maeda. 1997. Time-resolved Fourier transform infrared study of structural changes in the last steps of the photocycles of Glu-204 and Leu-93 mutants of bacteriorhodopsin. *Biochemistry.* 36:5134–5141.

Kandori, H., Y. Yamazaki, J. Sasaki, R. Needleman, J. K. Lanyi, and A. Maeda. 1995. Water-mediated proton transfer in proteins: an FTIR study of bacteriorhodopsin. *J. Am. Chem. Soc.* 117:2118–2119.

Kelemen, L., P. Galajda, S. Száraz, and P. Ormos. 1999. Chloride ion binding to bacteriorhodopsin at low pH: an infrared spectroscopic study. *Biophys. J.* 76:1951–1958.

Kono, M., S. Misra, and T. G. Ebrey. 1993. pH dependence of light-induced proton release by bacteriorhodopsin. *FEBS Lett.* 331:31–34.

Lanyi, J. K. 1993. Proton translocation mechanism and energetics in the light-driven pump bacteriorhodopsin. *Biochim. Biophys. Acta.* 1183: 241–261.

Lanyi, J. K. 1998. Understanding structure and function in the light-driven proton pump bacteriorhodopsin. *J. Struct. Biol.* 124:164–178.

Lanyi, J. K., and G. Váró. 1995. The photocycles of bacteriorhodopsin. *Isr. J. Chem.* 35:365–386.

Liu, S. Y. 1990. Light-induced currents from oriented purple membrane. I. Correlation of the microsecond component (B2) with the L-M photocycle transition. *Biophys. J.* 57:943–950.

Liu, S. Y., R. Govindjee, and T. G. Ebrey. 1990. Light-induced currents from oriented purple membrane. II. Proton and cation contributions to the photocurrent. *Biophys. J.* 57:951–963.

Liu, S. Y., M. Kono, and T. G. Ebrey. 1991. Effect of pH buffer molecules on the light-induced currents from oriented purple membrane. *Biophys. J.* 60:204–216.

Logunov, I., and K. Schulten. 1996. Quantum chemistry: molecular dynamics study of the dark-adaptation process in bacteriorhodopsin. *J. Am. Chem. Soc.* 118:9727–9735.

Lozier, R. H., R. A. Bogomolni, and W. Stoeckenius. 1975. Bacteriorhodopsin: a light-driven proton pump in *Halobacterium halobium. Biophys. J.* 15:955–963.

Luecke, H., B. Schobert, H.-T. Richter, J.-P. Cartailler, and J. K. Lanyi. 1999. Structure of bacteriorhodopsin at 1.55 Å resolution. *J. Mol. Biol.* 291:899–911.

Maeda, A. 1995. Application of FTIR spectroscopy to the structural study on the function of bacteriorhodopsin. *Isr. J. Chem.* 35:387–400.

Maeda, A., T. Ogura, and T. Kitagawa. 1986. Resonance Raman study on proton-dissociated state of bacteriorhodopsin: stabilization of L-like intermediate having the all-*trans* chromophore. *Biochemistry.* 25: 2798–2803.

Maeda, A., J. Sasaki, Y. Shichida, and T. Yoshizawa. 1992. Water structural changes in bacteriorhodopsin photocycle: analysis by Fourier transform infrared spectroscopy. *Biochemistry.* 31:462–467.

Mathies, R. A., S. W. Lin, J. B. Ames, and W. T. Pollard. 1991. From femtoseconds to biology: mechanism of bacteriorhodopsin's light-driven proton pump. *Annu. Rev. Biophys. Biophys. Chem.* 20:491–518.

Metz, G., F. Siebert, and M. Engelhard. 1992. Asp^{85} is the only internal aspartic acid that gets protonated in the M intermediate and the purple-to-blue transition of bacteriorhodopsin. A solid-state ^{13}C CP-MAS NMR investigation. *FEBS Lett.* 303:237–241.

Misra, S., R. Govindjee, T. G. Ebrey, N. Chen, J.-X. Ma, and R. K. Crouch. 1997. Proton uptake and release are rate-limiting steps in the photocycle of the bacteriorhodopsin mutant E204Q. *Biochemistry.* 36:4875–4883.

Needleman, R., M. Chang, B. Ni, G. Váró, J. Fornés, S. H. White, and J. Lanyi. 1991. Properties of Asp212→Asn Bacteriorhodopsin suggest that Asp212 and Asp85 both participate in a counterion and proton acceptor complex near the Schiff base. *J. Biol. Chem.* 266:11478–11484.

Oesterhelt, D., and W. Stoeckenius. 1971. Rhodopsin-like protein from the purple membrane of *Halobacterium halobium. Nature.* 233:149–152.

Otto, H., T. Marti, M. Holtz, T. Mogi, M. Lindau, H. G. Khorana, and M. P. Heyn. 1989. Aspartic acid-96 is the internal proton donor in the reprotonaion of the Schiff base of bacteriorhodopsin. *Proc. Natl. Acad. Sci. USA.* 86:9228–9232.

Otto, H., T. Marti, M. Holz, T. Mogi, L. J. Stern, F. Engel, H. G. Khorana, and M. P. Heyn. 1990. Substitution of amino acids Asp-85, Asp-212, and Arg-82 in bacteriorhodopsin affects the proton release phase of the pump and the pK of the Schiff base. *Proc. Natl. Acad. Sci. USA.* 87:1018–1022.

Petkova, A. T., J. G. Hu, M. Bizounok, M. Simpson, R. G. Griffin, and J. Herzfeld. 1999. Arginine activity in the proton-motive photocycle of bacteriorhodopsin: solid-state NMR studies of the wild-type and D85N proteins. *Biochemistry.* 38:1562–1572.

Rammelsberg, R., G. Huhn, M. Lübben, and K. Gerwert. 1998. Bacteriorhodopsin's intramolecular proton-release pathway consists of a hydrogen-bonded network. *Biochemistry.* 37:5001–5009.

Renthal, R., K. Shuler, and R. Regalado. 1990. Control of bacteriorhodopsin color by chloride at low pH: significance of the proton pump mechanism. *Biochim. Biophys. Acta.* 1016:378–384.

Richter, H.-T., L. S. Brown, R. Needleman, and J. K. Lanyi. 1996. A linkage of the pK_a's of Asp-85 and Glu-204 forms part of the reprotonation switch of bacteriorhodopsin. *Biochemistry.* 35:4054–4062.

Rodriguez, J., X.-Y. Yin, L. Villarreal, E. Rodriguez, R. Needleman, and R. Renthal. 1997. Long-range interaction between glutamic acid 74 and aspartic acid 85 in bacteriorhodopsin. *Biophys. J.* 72:A206.

Rothschild, K. J. 1992. FTIR difference spectroscopy of bacteriorhodopsin: toward a molecular model. *J. Bioenerg. Biomembr.* 24:147–167.

Scharnagl, C., J. Hettenkofer, and S. F. Fischer. 1995. Electrostatic and conformational effects on the proton translocation steps in bacteriorhodopsin: analysis of multiple M structures. *J. Phys. Chem.* 99:7787–7800.

Siebert, F., W. Mäntele, and W. Kreutz. 1982. Evidence for the protonation of two internal carboxylic groups during the photocycle of bacteriorhodopsin. *FEBS Lett.* 141:82–87.

Sonar, S., M. P. Krebs, H. G. Khorana, and K. J. Rothschild. 1993. Static and time-resolved absorption spectroscopy of the bacteriorhodopsin mutant Tyr-185→Phe: evidence for an equilibrium between bR570 and an O-like species. *Biochemistry.* 32:2263–2271.

Soppa, J., J. Otomo, J. Straub, J. Tittor, S. Meessen, and D. Oesterhelt. 1989. Bacteriorhodopsin mutants of Halobacterium sp. GRB. II. Characterization of mutants. *J. Biol. Chem.* 264:13049–13056.

Sperling, W., P. Carl, C. N. Rafferty, and N. A. Dencher. 1977. Photochemistry and dark equilibrium of retinal isomers and bacteriorhodopsin isomers. *Biophys. Struct. Mech.* 3:79–94.

Subramaniam, S., D. A. Greenhalgh, P. Rath, K. J. Rothschild, and H. G. Khorana. 1991. Replacement of leucine-93 by alanine or threonine slows down the decay of the N to O intermediates in the photocycle of bacteriorhodopsin: implications for proton uptake and 13-*cis*-retinal → all *trans*-retinal reisomerization. *Proc. Natl. Acad. Sci. USA.* 88: 6873–6877.

Subramaniam, S., T. Marti, and H. G. Khorana. 1990. Protonation state of Asp (Glu)-85 regulates the purple-to-blue transition in bacteriorhodopsin mutants Arg-82 → Ala and Asp-85 → Glu: the blue form is inactive in proton translocation. *Proc. Natl. Acad. Sci. USA.* 87:1013–1017.

Váró, G., and J. K. Lanyi. 1989. Photorections of bacteriorhodopsin at acid pH. *Biophys. J.* 56:1143–1151.

Váró, G., and J. K. Lanyi. 1991. Kinetic and spectroscopic evidence for an irreversible step between deprotonation and reprotonation of the Schiff base in the bacteriorhodopsin photocycle. *Biochemistry.* 30:5008–5015.

Zimányi, L., G. Váró, M. Chang, B. Ni, R. Needleman, and J. K. Lanyi. 1992. Pathways of proton release in the bacteriorhodopsin photocycle. *Biochemistry.* 31:8535–8543.

Zscherp, C., and J. Heberle. 1997. Infrared difference spectra of the intermediates L, M, N and O of the bacteriorhodopsin photoreaction obtained by time-resolved attenuated total reflection spectroscopy. *J. Phys. Chem.* 101:10542–10547.